Mean-field resonating-valence-bond theory for unpaired π-electrons in benzenoid carbon species

O. Ivanciuc, L. Bytautas,[a] and D. J. Klein[b]

Texas A&M University at Galveston, Galveston, Texas 77553-1675

A qualitative resonance-theoretic view is presented for the description of a variety of conjugated π-network species identified with "subgraphs" (either finite or infinite) of the graphite network. Within the framework of this resonance theory, simple rules are described to provide qualitative information: On ground-state spin multiplicities; on patterns of ground-state spin density; and on exchange splittings to low-lying "spin-flipped" excited states. Beyond ordinary benzenoid molecules, illustrative applications are noted to a diversity of extended species, including: Differently structured edges on semi-infinite graphite; corner structures where edges along different directions meet; conjugated polymer-strip ends; and local defect vacancy structures in extended graphite. The variety of simple resonance-theoretic predictions are compared against a semiempirical unrestricted Hartree–Fock view of some quantitative tight-binding molecular-orbital-theoretic computations. Agreement in predictions from the resonance- and band-theoretic viewpoints is taken to engender reliability of the so coincident predictions. A traditional organic chemical resonance-theoretic view is thence conveniently reformulated and brought to bear on several extended nano-structured systems to reveal systematic patterns of π-electronic behavior. © *2002 American Institute of Physics.* [DOI: 10.1063/1.1450547]

I. INTRODUCTION

The nature of π-electron networks has long been of interest, in providing the prototypical case of delocalized bonding, where there is more than one classical valence structure to describe the molecule. Indeed it was emphasized even before quantum mechanics that the structures of many benzenoid species were to be described simultaneously by a set of valence structures, without the compound exhibiting properties characteristic of what would have been surmised for a classical mixture. Perhaps this was most clearly said by Armit and Robinson,[1] but soon thereafter Pauling and Wheland[2] developed a quantum-mechanically based "valence-bond" (VB) approach to the phenomenon. But further they simplified[2] the result to a "resonance theory" making use just of the VB structures with a maximal degree of bonding and closely allied with the classical view. Then Pauling[3] went on to utilize an even simpler qualitative "enumerative resonance theory" as one of several new tools to understand a vast range of molecular structures, all as expounded in his masterwork *The Nature of the Chemical Bond*. And Wheland focused[4] on conjugated π-networks in organic chemistry, which is perhaps the most successful use of resonance theory, typically in a quite qualitative manner. And more recently Clar[5] developed the qualitative theory in terms of his "aromatic sextet."

Most of this resonance-theoretic work on conjugated π-networks has concerned nonradical species. But in fact one might imagine that this approach should be even more relevant in dealing with poly-radicals where the exchange-coupling between weakly paired electrons is central in characterizing these systems. Notably such poly-radical species have recently become of much interest in the area of "molecular magnetism."[6,7] When mixed ionicity or mixed valence is not dynamically involved one may often view the system as made up of interacting localized spins, and a Heisenberg-model description applies, most simply with just near-neighbor exchange couplings. Notably in physics there has been an on-going focus on such Heisenberg models to describe magnetic properties. Amusingly the Pauling–Wheland VB model[2] for conjugated hydrocarbons is in fact[8] naught but a Heisenberg spin Hamiltonian (though usually described in a somewhat different manner than is usually done in the physics literature on magnetism). It is perhaps surprising that the methods of the physics of magnetism then have not been extensively utilized in dealing with such organic conjugated molecules. But as it turns out the solution techniques developed in the traditional physics literature best apply to Heisenberg models for different structural circumstances, of high "coordination number" (and with antiferromagnetically signed interactions for cases of little "frustration"). For the case of low "coordination number" ($\leqslant 3$ for conjugated organics) solution methods *via* the resonance theory of Pauling and Wheland[2] turn out to be[9] more reasonable. Thus it is this resonance-theoretic approach that is pursued here, in application to organic species including those which at least are potentially radicaloid.

Quantitative approaches using the Pauling–Wheland VB model have often encountered computational difficulties. A number of VB-based approaches in chemistry largely ignore resonance-theoretic ideas, perhaps seeking to carry out con-

[a] On leave of absence from Institute of Theoretical Physics & Astronomy, Vilnius, Lithuania.
[b] Electronic mail: kleind@tamug.tamu.edu

figuration interaction computations over all covalent structures, with there already being ~ 100 for 10 π-centers and $\sim 10^4$ for 20 π-centers. Thence this brute-force approach becomes prohibitive beyond ~ 30 π-centers. But also there are a number of quantitative resonance-theoretic approaches[10–13] tending to restrict attention just to Kekule structures (i.e., exclusively neighbor paired structures), but not always. Still the numbers of such structures increase fairly rapidly with system size, so that (e.g.) there are $\sim 10^4$ Kekule structures for C_{60} buckminsterfullerene, and $\sim 10^6$ for typical C_{80} fullerenes. There have been some many-body resonance-theoretic computations even for extended systems (as reviewed in Ref. 14), and at a simpler level there has been rather much work[15] just enumerating Kekule structures. But these various resonance-theoretic developments have typically been somewhat special (often for selected nonradical species) and often are somewhat mathematically sophisticated (especially for larger systems). Indeed especially for extended systems it seems to have become the general belief that traditional organic qualitative resonance-theoretic ideas are out of their element.

Here a differently formulated qualitative "mean-field" resonance-theoretic approach is advocated, for application not only to ordinary benzenoid molecules but also to extended systems, including extended polymers, locally defected graphites, and graphitic edges. In this approach resonance structures are not restricted to be exclusively nearest neighbor paired, but in the mean-field approach the various resonance structures appear only implicitly. In the avoidance of reference to individual resonance structures, the exponential growth in numbers of such structures is side-stepped, so that even very large π-networks can be dealt with, even by hand, at least in a qualitative (or sometimes a semi-quantitative) sense. This mean-field resonance theory is described in Sec. II here, where the neat extension of traditional simple resonance-theoretic ideas is emphasized. The present predictions made *via* this approach concern the ground-state spin multiplicity, the general location of unpaired spin density, and the occurrence of low-lying excitations (as due to a weak spin-pairing between well separated electrons). The relations to more fundamental valence-bond Hamiltonians is considered in Ref. 16. And this resonance theory matches nicely to some earlier VB theorems which already quite successfully apply to smaller molecules (benzenoid or not). Thus here we choose to focus on its application and testing for extended nano-structured systems, different types of which are considered in Secs. III–VI. Notably real graphite is (e.g., as discussed in Ref. 17) quite rich in defects, often of ill-characterized structure, and a variety of conceivable such defects are treated here, as also are some conjugated polymer strips and other conjugated nano-structures. Section III applies our novel resonance-theoretic ideas to a variety of types of translationally symmetric graphitic edges, and then makes comparison to tight-binding band-theoretic results, such as have in fact already been a point of consideration in an earlier study.[17] Here the checking against computations based on a molecular-orbital (MO) view is more completely done (and some of the particular insights developed here are utilized in later sections). Section IV goes on to apply our

resonance-theoretic ideas to a selection of "corners" on graphitic edges, Sec. V applies the ideas to different types of ends of a long polymer strip, and checks are made against (brute-force) MO-based computations. Section VI addresses the question of vacancy defects in the graphitic π-network. This is neatly explicated in terms of "anti-molecules" (each anti-molecule corresponding to the molecule comprised from the set of π-centers deleted from the lattice). Again checks are made against somewhat more involved MO-based computations. With the successful comparisons it thus seems that the proposed qualitative mean-field resonance theory offers ready insight, building on traditional chemical resonance-theoretic ideas, revealing patterns of behavior, and exhibiting a range of potential applications, to a variety of nano-structures, even defected extended systems, which are oft otherwise difficult to deal with theoretically. The ideas thence extend traditional organic chemical reasoning to encompass some applications often associated with physical chemistry, and therefore the ideas seem of potential interest for a wide audience of chemists.

II. MOLECULAR-FIELD RESONATING VB THEORY

The use of resonance theory in a qualitative[4,5] or quantitative[10–15] manner has been applied most widely for stable nonradical species. As already noted Pauling's simple resonance theory is based upon the consideration of sets of different classical chemical-bonding patterns consistent with the considered molecular graph. For our considerations this molecular graph should preferably have few nearest neighbors, as is the case for conjugated hydrocarbons. For the (neutral) benzenoids there is one π-electron per site, and there are exchange couplings between the electrons on these different neighbor sites. To each bonding pattern there is imagined a basis wave function Φ with *singlet spin pairings* (corresponding to π-bonds) of the π-electrons on the sites interconnected in the bonding pattern. The more important individual bonding patterns are usually those with a greater number of neighbor spin pairings (giving lower energies over the VB exchange-coupling Hamiltonian). Further the greater the number of low-energy such VB patterns Φ, the greater the stabilization (because of mutual "configuration" interaction amongst them), this phenomenon being termed *resonance*. But even patterns with non-neighbor pairing can contribute to this resonance especially if first they are not too different from a maximally neighbor-spin-paired pattern and second there are a great number of such structures. Thus to achieve overall energetic stability the tendencies first to maximize the number of neighbor-paired sites and second to maximize the number of resonance (or VB) structures often are in competition. Generally there is some contribution from non-neighbor bonding, and in some cases this may even be dictated by the molecule (being without a fully neighbor-paired VB structure). But as an extension to the preference to neighbor pairing there is a secondary preference to a slightly more distant local "vicinity" pairing. If pairing between very distant sites makes a contribution, then the spin pairing is weak in the sense that at a very slight energy above the ground-state there should be a state with the electron pair
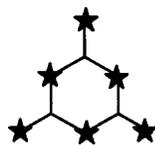
FIG. 1. An assignment of stars and unstars to the carbon atoms of 1,3,5-trimethylene-benzene.

FIG. 2. Pauling bond orders and free valences for benzene, naphthalene, and trimethylene-methyl.

truly unpaired—i.e., an excited state with additional unpaired spin density and an overall spin greater by 1 than the ground state.

These general ideas can be given more substance for the case of *alternant* systems G, these being those with a conjugated π-network which may be partitioned into *starred* and *unstarred* sets A and B of sites, such that each such type of site has nearest neighbors which are solely of the other type. Thence, e.g., for 1,3,5-trimethylenebenzene one has starred and unstarred sites as indicated in Fig. 1. Now it is crucial in our considerations that any non-neighbor pairing may be stipulated (in the ground state) to occur solely between sites in the *starred* and *unstarred* subsets. As long ago noted,[18] a double spin-pairing one within A and one within B may be reexpressed as a linear combination of two inter-set double spin-pairings. Note that VB functions with an intra-set spin-pairing do not gain energy-stabilization, since there are no intra-set (antiferromagnetic) exchange couplings in the bipartite network G, and such spin-pairing introduces constraints on the function which otherwise would be absent. There are a couple different standard[19,20] bases of VB functions of suitable (ground-state) spin designated with spin-pairings solely between the sets A or B. Thence it seems that the ground state for bipartite G should have no such intra-set spin-pairings.

The question of the competition between maximization of neighbor pairing and resonance may be rephrased in terms of "bond orders" and "free valences." The *resonance bond order* for a neighbor pair e of sites is putatively identified as the fraction p_e of ground-state contributing structures which have the π-electrons on these two sites spin-paired; and the *free valence* for a π-center i is the fraction v_i of ground-state contributing structures which have no spin-pairing to another π-electron in the vicinity of site i. What is meant by "vicinity" here may be given different interpretations. If the vicinity is taken as the limit of nearest neighbors with all spin-pairing between such neighbors (and each of the maximally spin-paired bonding patterns is taken to contribute equally to the ground state), then the p_e are called[21] *Pauling bond orders*, and the associated v_i might be called *Pauling free valences*. For instance, in Fig. 2 Pauling bond-orders and free valences for three molecular species G are indicated. It has been demonstrated[22,23] that for a variety of nonradicaloid benzenoids the Pauling bond-orders correlate closely with experimental bond lengths. But we do not restrict attention to nonradicals or limit spin-pairing to near neighbors. Any remnant free valence may be indicative of unpaired spin density, as in the third case of trimethylenemethane in Fig. 2. The prediction here of two unpaired electrons with spin density primarily on the end atoms is known in agreement with
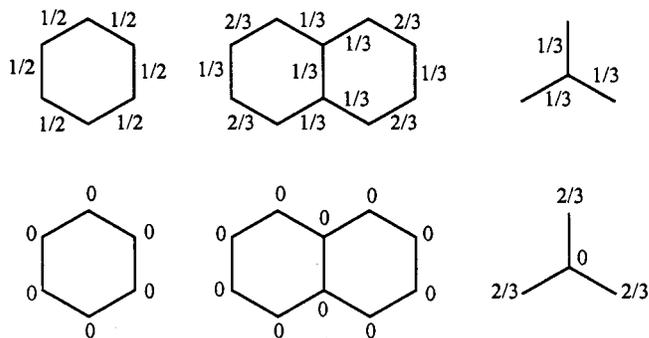
experiment[24] and high-quality *ab initio* computations.[25] A primary difference from the traditional use of Pauling bond orders is that we develop the bond orders and free valences without explicit generation of the various resonance-structures.

The maximization of the number of neighbor-paired sites clearly minimizes the free valences. The maximization of resonance is also somewhat intuitively clear: Resonance is greatest when the bonding patterns are as delocalized as possible. That is, for maximal resonance one might anticipate that the probability (or bond-order) of a double bond along any one of the directions away from a site to its nearest neighbors is equally likely. For benzenoids the maximum number of neighbors is 3 so that resonance would seem greatest the more nearly the π-bond orders are to 1/3. Then even without explicit consideration of the Kekule structures of a species, the maximization of resonance might lead one to (tentatively) assign *zeroth-order* bond orders of 1/3 and corresponding *zeroth-order* free valences as deficits of the sums of these zeroth-order bond orders incident at a site. That is, this zeroth-order free valence for a site i turns out to be just the deficit from 1 of one-third of the degree of site i. In many cases additional pairing between neighbor sites may further reduce the free valences, yielding *first-order* bond orders and *first-order* free valences. Thence such first-order free valences for the species of Fig. 2 turn out to be the same as the Pauling values already illustrated. For G being 1,3,5-trimethylene-benzene the zeroth-order free valences turn out as in Fig. 3, whereas the Pauling free valences (obtained by generating and examining the 18 nearest-neighbor resonance structures) turn out to be slightly different as also indicated in this figure. Finally shown in this figure are the spin densities for the spin-quartet wave function built from the Hückel MOs. Evidently the three sets of values are qualita-
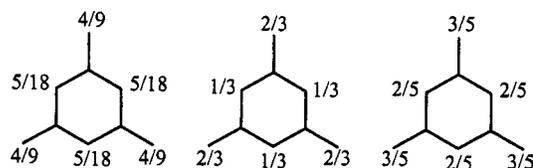

FIG. 3. Pauling free valences for 1,3,5-trimethylene-benzene, resonant-theoretic zeroth-order free valences, and finally Hückel-Hund spin densities (for the same tri-radical).

tively (and even semiquantitatively) similar, all having no spin density on the minority type (unstarred in Fig. 1) of sites.

Now one may introduce additional pairing between starred and unstarred sites even if not a neighbor (though preferably as close as possible). That is, the first-order free valences are (at least partly) satiated by other more distant free valences located on the other type of sites (i.e., starred versus unstarred sites). As a consequence it is just the difference between the net free valences in the A and B sets which results in globally unpaired spins (in the ground state). That is, the overall ground-state spin is predicted to be given in terms of the free valences v_i as

$$S_{RT} = \left| \left\{ \overset{\star}{\sum_i} v_i - \overset{\circ}{\sum_j} v_j \right\} \right| \Big/ 2. \tag{1}$$

This predicted ground-state spin turns out[17,26] to be independent of details of the definition of the v_i (just so long as they are deficits of the bond orders from 1). Indeed using the zeroth-order estimates this spin can be re-expressed in terms of the numbers $\#_{\star n}$ of starred sites of degree n and the numbers $\#_{\circ n}$ of unstarred sites of degree n, thusly

$$S_{RT} = |2\#_{\star 1} + \#_{\star 2} - 2\#_{\circ 1} - \#_{\circ 2}|/6, \tag{2}$$

Notice too that the (unpaired-electron) spin density should appear primarily on the sites with more free-valence. If the free valences only become small (perhaps 0) at high order (*via* pairing between more well separated opposite-type sites), then there are predicted to be low-lying states with these high-order spin pairings absent.

An aside of note is that the prediction of Eq. (1) for finite alternants persists beyond simple resonance theory, to the nearest-neighbor Heisenberg spin Hamiltonian (for spin $s = 1/2$ sites) on the full space of all (homopolar) covalent structures. Indeed, if one notes that the numbers of bonds exiting from $\star$ and $\circ$ sites must match, then the resonance-theoretically predicted ground-state spin may be reexpressed in terms of just the total numbers $\#_\star$ and $\#_\circ$ of starred and unstarred sites

$$S_{RT} = |\#_\star - \#_\circ|/2, \tag{3}$$

such as is known to hold for the more "complete" nearest-neighbor Heisenberg model,[27–29] as well as the even more complete Hubbard model[30] for these same systems. And the results seem always to be in agreement[31] with full configuration-interaction computations on more conventional PPP models. For the nearest-neighbor ($s = 1/2$) Heisenberg model there are some further qualitative theorems[32] which seem also typically to be consistent with our current results concerning the location of the unpaired spin density. And there are a number of *ab initio* computations with which agreement is obtained—see, e.g., Ref. 33. With this earlier noted dove-tailing with previous VB-theoretic work for finite molecules, it is natural to next address extended systems, where the present approach promises to be able to deal with local features, and even identify pairings so weak that they are typically better viewed as unpaired.
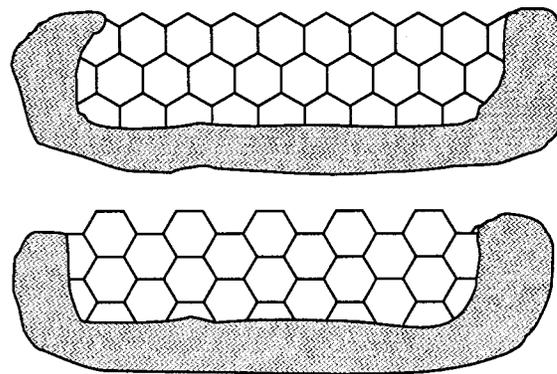

FIG. 4. Portions of two types of translationally symmetric edges for semi-infinite graphite. The blackened area is understood to contain further network continued in the natural fashion.

III. TRANSLATIONALLY SYMMETRIC GRAPHITIC EDGES

For the case of translationally symmetric edges, our resonance-theoretic approach quite easily makes predictions, about the number of unpaired spins per unit cell of edge. For instance, for the two types of edges in Fig. 4 one may apply the resonance-theoretic arguments to reveal 1/3 of an unpaired electron per unit cell in the first (zig–zag) case, or 0 in the second (corrugated) case. The first-order bond orders and unpaired spin densities for a single unit cell are given in Fig. 5, where also the analysis is repeated for a third type of edge, with a resultant 2/3 of an unpaired electron per unit-cell length of edge. In Fig. 6 we indicate unit cells for a more comprehensive list of about two dozen possible edges, and the zeroth-order free valences are indicated there along with additional low-order spin pairings. Evidently the predictions are quite readily made, though a question of their reliability arises.

One test of the predictions made in the preceding paragraph would be *via* Hartree–Fock (HF) or unrestricted HF computations on these systems with such edges. Most feasible would be such quantum chemical computations on wide strips with two edges but well separated from one another, so that there would be little "communication" between opposite edges. In such a case with (wide) strips there would be just a finite number of sites per unit cell, thereby facilitating ordinary band-theoretic computations. The restricted
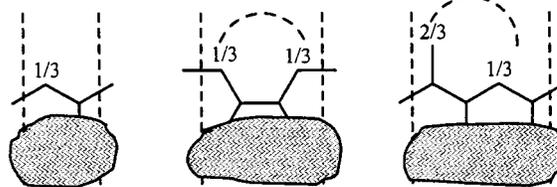

FIG. 5. Unit cells of edge for three types of edges (including the two of Fig. 4), with the vertical dashed lines indicating boundaries of the unit cell, which continues on downward into bulk graphite. The zeroth-order free valences which are nonzero are shown, and curved dashed lines for the second (corrugated) and third cases indicate first-order pairings, whereafter the first-order free valences would be 0 for the second case, while for the third case there would remain a free valence of 1/3 of an electron per unit cell of edge.
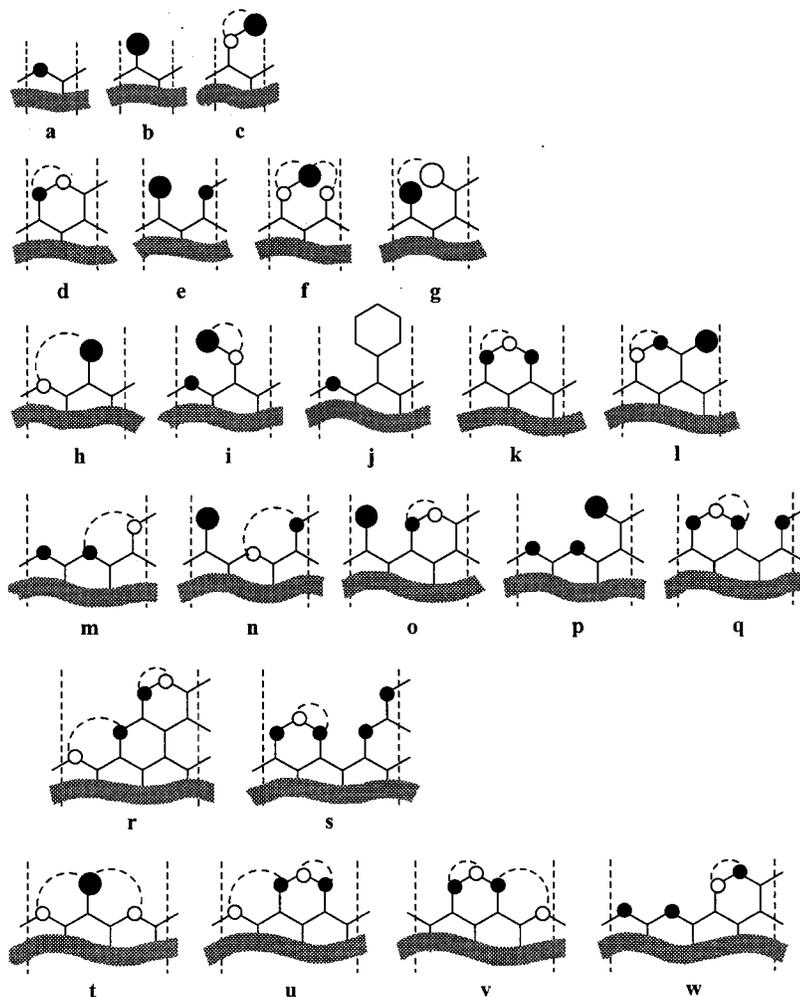
FIG. 6. Unit cells of about two dozen types of edges showing zeroth-order free valences encoded with values of 1/3 and 2/3 represented by small and large circles, with the circles being filled or empty as the site is starred or unstarred. The curved dashed lines in some cases indicate higher-order spin pairings.

HF solutions (for uniform bond-length) PPP models are equivalent to the solution of the simple Hückel model, and the ensuant occurrence of certain unrestricted HF solutions can be readily recognized. First, for alternant systems there is[34] a (fairly well-known) "pairing" symmetry in the eigenvalue spectrum about the nonbonding energy here taken as 0. This symmetry is that for every eigenvalue ϵ there is a corresponding eigenvalue $-\epsilon$. So if there are Hückel molecular orbitals (MOs) which are only very weakly bonding (i.e., MOs with very small magnitude negative ϵ), then there are corresponding very weakly anti-bonding MOs. As a consequence in such a circumstance, there is a UHF instability for the associated PPP model, where the weakly bonding and anti-bonding MOs mix and end up being singly occupied [rather than in the restricted Hartree–Fock (RHF) approximation solely the bonding MOs being occupied, with the occupancy being double]. Indeed this UHF instability is[17,35] very easy to understand in that if the ϵ are very small in magnitude, then it costs little orbital energy to so redistribute the electrons, while an exchange-energy stabilization (proportional to the electron–electron interaction strength) results. Whether such a unrestricted Hartree–Fock (UHF) stability occurs of course depends on just exactly how small ϵ is in magnitude (as well as on some details of the exchange interaction for the indicated orbitals). But as it turns out[17] for suitable strips of width w there often are a "flock" of edge

states with $\epsilon \approx Ce^{-a/w}$, so that for the limit of wide strips it is assured that this ϵ becomes small enough in magnitude for the UHF instability to occur. Moreover, these edge-localized incipiently singly occupied MOs are easy to recognize just from an energy-band diagram, because they must occur in a region of this diagram different than the MOs of bulk edgeless graphite which has[36] a 0 density of MO levels at the nonbonding energy. That is, if there are a substantial number of edge-localized incipiently singly occupied MOs (associating to unpaired electrons), then in a standard MO band diagram they should occur as portions of otherwise absent bands very near to $\epsilon=0$. Several such band diagrams for strips (of widths all taken $w \geq 30$) are shown in Fig. 7. These plots are for discrete sets of (~ 25) wave vectors k between 0 and π (it being understood that for k between $-\pi$ and 0 the result is just the same as already shown with a reflection in a vertical plane at $k=0$). In all these cases the bulk of the bands all fall into a shaded region (shaded because of the density of MO-energy points) corresponding to what occurs with bulk (edgeless) graphite. But in many of these cases there are bands which penetrate out of the shaded region and hug to a portion of the nonbonding k axis of $\epsilon=0$, it being these exceptional MOs which must be the edge-localized nonbonding ones. If the portion of such an $\epsilon=0$-hugging band covers a fraction f of the Brillouin zone, then this cor-
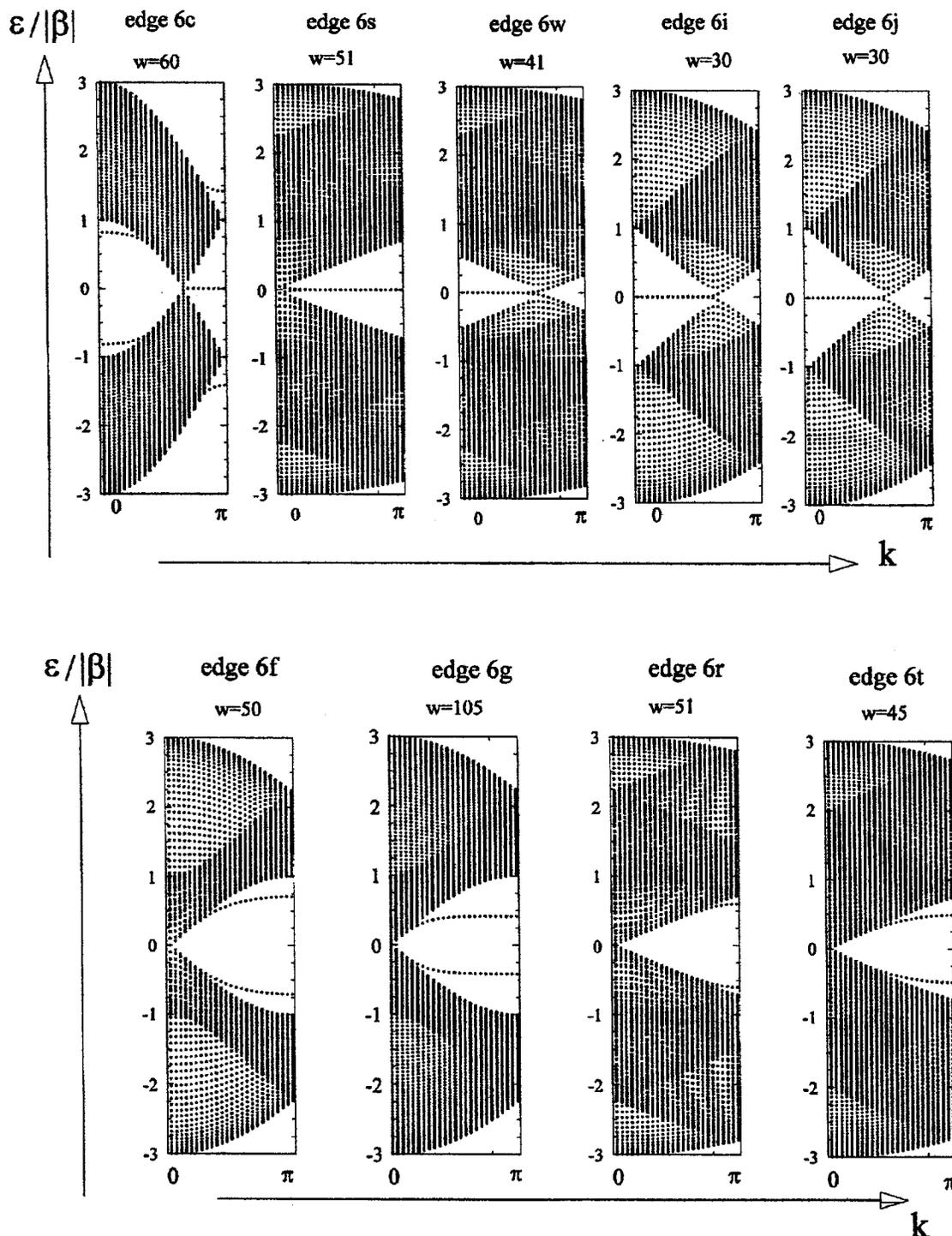
FIG. 7. Energy level diagrams (in the right half of the first Brillioun zone) for several edges identified to their unit-cell diagrams of Fig. 6. Those in the first row all exhibit an asymptotically nonbonding portion of a band penetrating outside the otherwise densely occupied part of the Brillouin zone. Those in the second row all exhibit no nonbonding orbitals except at $k = \pm 2\pi/3$, to give no unpaired-electron-spin density.

responds to f unpaired electrons per unit cell. As a test of these edge-localization features, Fig. 8 illustrates the logarithms of the mean densities of several such MOs as a function of their distance from the edge of Fig. 6(j). For such orbitals the density is seen to fall exponentially with the distance d from the (nearest) edge, though the exponential fall-off rate is seen to be different for different k values. The edge-localization is seen to be more severe the greater the distance in the Brillouin zone of the near-nonbonding MO is

from those for bulk-graphite MOs (in the "shaded" regions). The MOs in the shaded regions are more or less uniformly spread across the strip.

Now we have predictions for the number of unpaired electrons per unit cell of edge, both by the resonance-theoretic approach and by an MO-theoretic computation. Only some of the MO computations are indicated in Fig. 7, with results of some other computations available in earlier articles.[17,37–39] The consequent RVB-theoretic predictions for

J. Chem. Phys., Vol. 116, No. 11, 15 March 2002

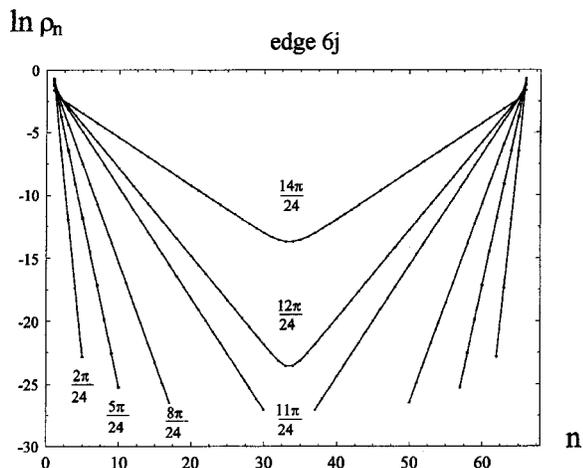Resonating valence bond theory   4741

FIG. 8. Logarithmic mean electron density plots as a function of position across a strip for various MOs of the exceptional (near) nonbonding MO band for the case of the edge of 6(j). The different curves are for different band orbitals at the indicated different wave vector values k.

the number $\#_u$ of unpaired electrons per unit-cell of length are given in Table I for the two dozen edges indicated in Fig. 6. Table I also identifies the *primitive translation* (x,y) associated with each type of edge, where this (x,y) indicates a step of x hexagons along one direction and y hexagons in the direction 60° counter-clockwise to the first direction carries an edge back into itself. (As an aside we may note that given this (x,y) label for an edge it may be shown[17] that $\#_u$ is integer iff x-y is a multiple of 3, and in particular there can be no unpaired electrons only if x-y is a multiple of 3.) Finally in Table I references dealing with the various cases from the band-theoretic viewpoint are indicated, with the parenthetic

TABLE I. Edge symmetries and edge-localized unpaired electrons per unit cell of edge.

Structure in Fig. 6	Primitive translation (x,y)	Unpaired electrons $\#_u$	Band theory references
(a)	(1,0)	1/3	17, 37
(b)	(1,0)	2/3	36
(c)	(1,0)	1/3	17, here
(d)	(1,1)	0	38, 39
(e)	(1,1)	1	17
(f)	(1,1)	0	here
(g)	(1,1)	0	here
(h)	(2,0)	1/3	17
(i)	(2,0)	2/3	17, here
(j)	(2,0)	2/2	17, here
(k)	(2,0)	1/3	17, 39
(l)	(2,0)	2/3	17
(m)	(2,1)	1/3	17, 39
(n)	(2,1)	2/3	
(o)	(2,1)	2/3	
(p)	(2,1)	4/3	
(q)	(2,1)	2/3	
(r)	(2,2)	0	here
(s)	(2,2)	1	here
(t)	(3,0)	0	17, here
(u)	(3,0)	0	17
(v)	(3,0)	0	17
(w)	(3,1)	2/3	39, here

references indicating some partial theoretical treatment, short of the computations such as reported in Fig. 7. Notably there is unanimous quantitative agreement between $\#_u$ (from our resonance theory) and the number $\#_{NBMO}$ of nonbonding electrons per unit cell of edge length (from the band-theoretic computations). That is, we find

$$\#_{NBMO} = \#_u, \tag{4}$$

for all translationally symmetric edges considered, including not only the nine representative cases of Fig. 7, but in fact all others occurring in Table I. Further it turns out (as indicated in Fig. 8) that there seems to be qualitative agreement as to the location of the unpaired electrons. Here in Fig. 8 the densities ρ_n for an orbital of different indicated k from the exceptional band are plotted as a function of position n, and to suppress oscillations (between ★ and ◯) ρ_n at a distance $n=d+1/2$ from the edge is taken as the sum of the squares of orbital coefficients at the sites at distances d and $d+1$ from the edge. The resonance theory evidently reveals an interesting pattern of behavior, giving ready insight into interesting chemico-physical characteristics of the various edge structures.

It is to be emphasized that the edge-localized electrons should be crucially important for magnetic susceptibilities and electrical conductivity. These electrons which are unpaired within a first approximation, still do exchange couple amongst one another, presumably with a ferromagnetic sign, so that they would be very important for the bulk magnetic susceptibility, even though the edges are a small fraction of the total. With the edge-localized orbitals singly occupied and located at the Fermi energy, electrical conductivity may be much enhanced—it being well-known that bulk (edgeless) graphite though having 0 band gap also has[36] a 0 density of states at the Fermi surface. To deal with such properties in more detail a quantitative treatment would be best.

IV. GRAPHITIC CORNERS

The general resonance-theoretic argument is readily applicable to treating corners on large graphitic fragments. Of course unpaired electrons at corners are more noticeable if the edges meeting at the corners are of the type which do not themselves lead to edge-localized unpaired electrons, one such being the "corrugated" edge of the second part of Fig. 4. Then for instance, for the four corners of Fig. 9 we predict no edge-localized unpaired electrons for the first two cases, while the last two cases are somewhat more complicated. For these last two cases one sees that full spin-pairing beyond that of zeroth-order may be achieved, though in these there are a number of pairings of a more distant nature, so that these pairings are somewhat weak. Throughout all of the cases of Fig. 9 the curved dotted spin-pairings are taken to indicate 1/6 spin-pairing bond orders, so that two sites connected by two such curved dotted spin-pairings exhibit 1/3 spin-pairing bond order between the two sites. Evidently the fourth case of Fig. 9 exhibits more rather distant weakly paired electrons than the third case, while the first two cases exhibit even less of such more distant pairing. It is seen that the different edges meeting at a corner allow electrons at the corner to pair along the edges on each side of the corner
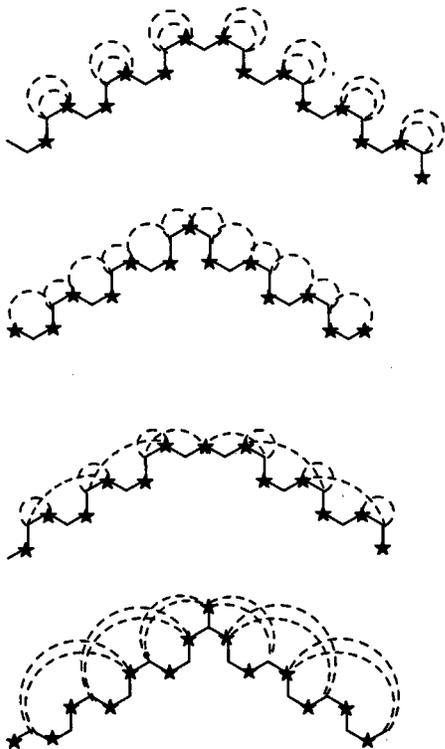
FIG. 9. Four graphitic corners, showing zeroth-order free valences and additional higher-order spin pairings. Note that each dashed line is a spin pairing beyond zeroth-order, with the convention taken here that each such dashed line contributes 1/6 to the indicated bond order.

while displacing some local pairings along the edge to more distant pairings farther along the edge. For more quantitative predictions a more quantitative approach would be desirable.

Again one may test these qualitative predictions against those from an MO-theoretic approach. In this case to make the requisite computations it seems convenient to deal with finite but large molecular fragments with the indicated types of corners. And again it is expedient to compute within a restricted HF result, it being understood that very slightly bonding restricted-HF MOs would for a related unrestricted HF approximation mix with corresponding weakly antibonding MOs and end up being singly occupied (i.e., unpaired), following the general discussion in Sec. III. Thus for
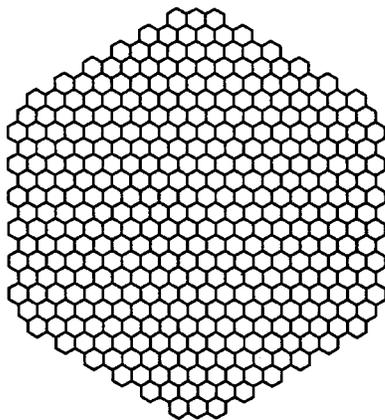

FIG. 10. A large hexagonal-symmetry fragment of graphite with $N=834$ sites and graphitic corners of the third type shown in Fig. 9.
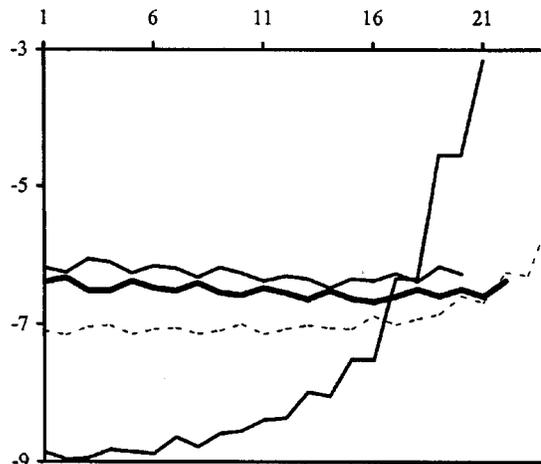

FIG. 11. HOMO (or near-HOMO) densities for the corners of Fig. 9. The first, second, third, and fourth corners of Fig. 9, respectively, correspond to: The lighter-face slightly higher near-level curve; the bold-face slightly lower near-level curve; the dashed curve which changes somewhat more; and the bold-face curve which changes most dramatically.

the first type of corner we might try computations on a hexagonal-symmetry fragment as indicated in Fig. 10. Similar hexagonal-symmetry fragments are possible for each of the three other corners of Fig. 9. If the MO approach finds a number n of (near) nonbonding MOs, then we would have $n/6$ per corner. But because the fragments are finite the unpaired density our resonance-theoretic argument associates to each corner might end up (in the resonance-theoretic picture) pairing weakly with requisite others down the adjacent edges displacing what would otherwise being near-neighbor pairings along the edges to more distant pairings. Within the MO picture, the orbitals would not then be expected to be quite nonbonding (much as for the edge-localized MOs on finite strips of not too great of a width). Thus for the four corners of Fig. 9 we have carried out computations on four hexagonal-symmetry fragments of $N=684$, $N=546$, $N=834$, and $N=552$ sites. The nth unoccupied MO above the nonbonding 0 is denoted ϵ_n, so that the highest occupied molecular orbital–lowest unoccupied molecular orbital (HOMO–LUMO) gap would be $2\epsilon_1$. Then these lower-lying such energies for the three indicated fragments, respectively, are (measured in units of magnitude of the Hückel resonance integral β)

	9(a)	9(b)	9(c)	9(d)
ϵ_1	(0.1196)	(0.1362)	0.0807	0.0078
ϵ_2	(0.1196)	(0.1362)	0.0807	0.0087
ϵ_3			(0.1128)	0.0087
ϵ_4				(0.1448)

where the (left-to-right) order of these orbital energies corresponds to the order of the edges in Fig. 9, and the parenthetic values identify MOs which are here considered as outside the (weakly) non-bonding range. Conditionally identifying those MOs of energy $\epsilon_i \lesssim 0.010$ as nonbonding, we see that their number for our four fragments then is 0, 0, 4, and 6, which is in rough agreement with our qualitative resonance-theoretic predictions of 0, 0, m, and n (nearly) unpaired electrons per
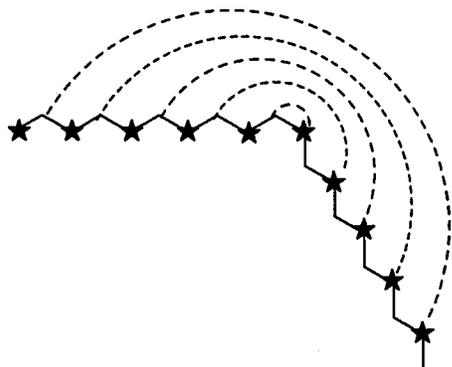
FIG. 12. A graphitic corner where two zig–zag edges meet. The spin-pairing around the corner is seen to pair ever more distant sites.

corner, with $m < n$, and the values of m and n dependent on what one means by "weak" pairing. Now in Fig. 11 we show logarithms of the mean densities of the more nearly non-bonding HOMOs at a distance d from the hexagonal center of the molecular fragment. As in the discussion of the edges the density ρ_d for position d is averaged between the densities at $d - 1/2$ and $d + 1/2$, so that oft sizable oscillations of the densities between ★ and ○ sites are averaged out. The HOMOs for the first two cases of Fig. 9 seem from Fig. 11 not to be corner localized but spread out throughout the fragment. For the third case of Fig. 9 the logarithms of the average densities for the two weakly bonding MOs is plotted in Fig. 11, and it is seen that they are evidently corner localized. For the fourth case of Fig. 9 we have plotted the logarithm of the sum of the densities for the three weakly bonding MOs, and it is seen that they appear to be corner localized. The orbitals which we have conditionally identified as "nonbonding" on the basis of their energies ($\epsilon_i \lesssim 0.010$) are thence seen from Fig. 11 to appear to be localized at the outer reaches of the fragment, and appear to have a density decay into the interior roughly of an exponential fashion. Presum-

ably for even larger fragments the decay would presumably continue to ever smaller densities at ever greater distances from the corners.

Not only may corners introduce unpaired electrons, but they may also cause pairing between electrons on two adjacent edges which would otherwise be unpaired. For instance, for (polyacenoid) zig–zag-type edges meeting at a corner as in Fig. 12 we have already seen in Sec. III that these edges in isolation should have 1/3 of an unpaired electron per zig–zag unit of edge, while from Fig. 12 we see that there can be pairing around the corner. But in order to achieve pairing for the otherwise unpaired edge electrons far from the corners the distance of the pairing becomes quite large, and therefore, quite weak. Thus some of these electrons remain in essence unpaired, though what we really have is a gradation of pairing strengths, and associated degrees of localization. If we carry out an MO computation for a hexagonal-symmetry fragment with six such corners and $N = 1014$ sites, we find (in units of $|\beta|$)

$$\epsilon_i = 0.0055, \quad 0.0055, \quad 0.0063, \quad \text{for} \quad i = 1-3,$$

$$\epsilon_i = 0.0299, \quad 0.0299, \quad 0.0342, \quad \text{for} \quad i = 4-6,$$

$$\epsilon_i = 0.0831, \quad 0.0831, \quad 0.0976, \quad \text{for} \quad i = 7-9,$$

$$\epsilon_i = 0.1551, \quad 0.1551, \quad 0.1899, \quad \text{for} \quad i = 8-11.$$

That is, we do indeed find the predicted gradation of MO energies away from the nonbonding value of $\epsilon = 0$. Moreover, in Fig. 13 we consider the densities for the first three sets of triples orbitals as averaged over the three similar-energy orbitals in each set, plotting the logarithms of these average densities as a function of the distance from the center of the fragment. It is seen that the sets of more nonbonding orbitals are more edge localized, again nicely matching with the resonance-theoretically anticipated gradation.

V. POLYMER-STRIP ENDS

Polymers being of finite length typically have ends where the erstwhile (near) translational symmetry is strongly broken and something special may happen. If the question of end-localized unpaired spins is to be considered, then this will be simplest if the edges along the polymer length are such as not to tend to introduce unpaired electrons, and thereby interfere with any possible unpaired electrons at the ends. Thus we might consider a long polymer strip with "corrugated" edges [as in Fig. 4(b)] and a width of one hexagon, it happening that such polyphene chains are beginning to be experimentally realized.[40] Then one may imagine numerous possible ends, four of which are indicated in Fig. 14. Our resonance theory readily leads to predictions of 0, 1, 1, and 0 unpaired electrons for the respective ends of Fig. 14.

These predictions may be checked against Hückel MO computations for fairly long oligomers of 100 hexagons in length. The consequent logarithms of the HOMO densities measured from the strip end are indicated in Fig. 15. These computations are for strips with both ends of such an oligomer of the same type, and the densities averaged over the sites of a hexagon are reported as a function of the position
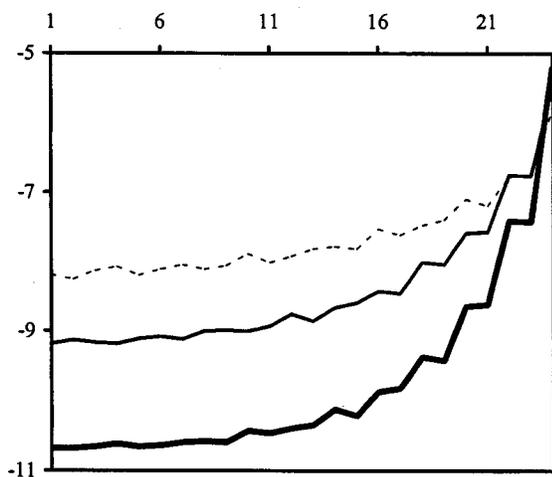

FIG. 13. Near-HOMO orbital mean densities measured from the center of a hexagonal fragment with 6 like corners of one of the types in Fig. 12. The bold line is for the first triplet of orbitals, the fainter line is for the second triplet, and the dashed line is for the third triplet.
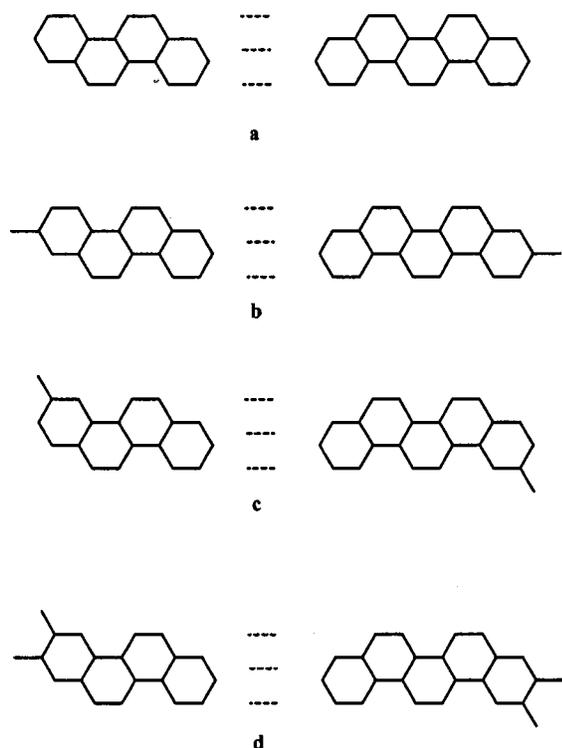
FIG. 14. Four types of polymer strip ends for a phenanthrenoid polyphene polymer.

of the hexagon along the strip. The first and last cases evidently have the frontier-orbital energy ϵ_1 notably displaced from 0, to $\epsilon_1 = 0.382\,72$ and $\epsilon_1 = 0.190\,77$, respectively, whereas the second and third cases have the frontier-orbital energies ϵ_1 and ϵ_2 very nearly 0, to within less than 10^{-14}, so that the observed numbers of (very) weakly bonding MOs turns out for our four considered cases to be 0, 2, 2, and 0. The corresponding frontier-orbital densities in the first case
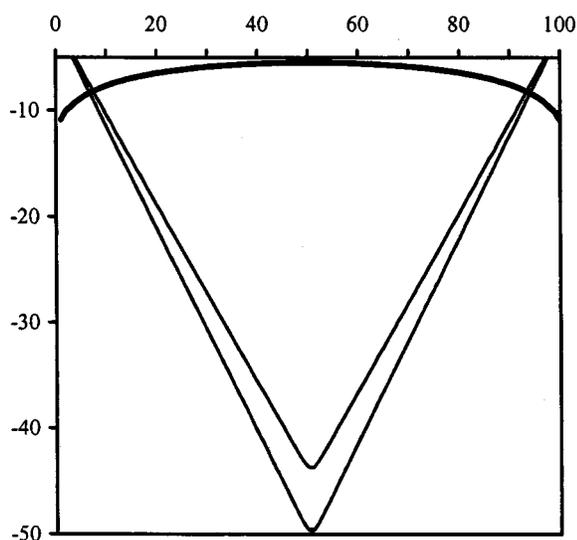

FIG. 15. Logarithmic mean HOMO (or near-HOMO) densities as a function of position along the polymer strip for the four types of strip ends of Fig. 14. The first case of Fig. 14 gives the relatively level curve (for logarithmic values between −5 and −11. The second and third cases give quite similar solid vee-shaped curves which on our present plot cannot be clearly distinguished, and the fourth case gives the dashed vee-shaped curve.

is seen from Fig. 15 to be quite delocalized. The frontier-orbital densities for the second and third cases are very similar being indistinguished in the figure and corresponding to the lowest (solid) curve—evidently these orbitals are end localized as expected, and even strongly end-localized, with a smooth exponential fall-off to the center of polymer chain. The fourth case involves an apparently doubly degenerate orbital and corresponds to the dashed curve in Fig. 15—it evidently is also end localized, though this does not correspond to unpaired electrons since the orbital energy is such as to distinguish it quite clearly from being nonbonding (or even nearly nonbonding). It may be mentioned that in dealing with graphitic edges (as in Sec. III) there occasionally too are edge-localized orbitals which are not nonbonding [and seem to be easily recognized as exceptional nonbonding bands penetrating out of the shaded regions, as in Figs. 7(f)–7(h)]. That is, it seems that the prediction of localized unpaired electrons via resonance theory is sufficient (but not necessary) for the existence of nonbonding MOs. It is an interesting question as to whether the qualitative resonance theory might turn out to predict the localized but bonding–anti-bonding orbitals as in the case of the fourth end of Fig. 14 (say perhaps because the Kekule structures one can write down for this end have localized double bonds for the double bonds near the ends of the oligomer strip), but here we do not seek to develop this aspect. For our polyphene polymer strips evidently there is notable agreement between resonance- and MO-theoretic predictions (for end-localized unpaired electrons and end-localized nonbonding MOs, and consequent electrons).

It may be noted that for some cases what goes on at the polymer ends may be more intimately mixed up with the nature of the edges. First if there are unpaired electrons along the length of the polymer, then they would be in nearly nonbonding MOs delocalized along the length and able to intermix with nearly nonbonding MOs initially assigned to the polymer ends, so that none of the eigen-MOs might be end localized. Further, some edges may exhibit a sort of balance regarding formation of unpaired electrons, so that they would arise under some very slight perturbation. Notably this circumstance of "balance" is not overly rare, and has to do with whether lone solitonic excitations occur (in the neutral conjugated network). These considerations are best approached with a little more quantitative detail, and has been so discussed elsewhere[41] (paying explicit attention to Kekule structures), and also are empirically found to correlate with MO-based results. We do not pursue this interesting aspect further in our present qualitative discussion.

The indicated tests concerning corner and end structures show quite reasonable agreement between the predictions of the resonance-theoretic approach and of the MO-theoretic approach. The main qualification relates to interactions between different near-by edges, whence a quantitative resonance-theoretic modeling (or a quantitative MO-theoretic modeling) may be needed to make better predictions.
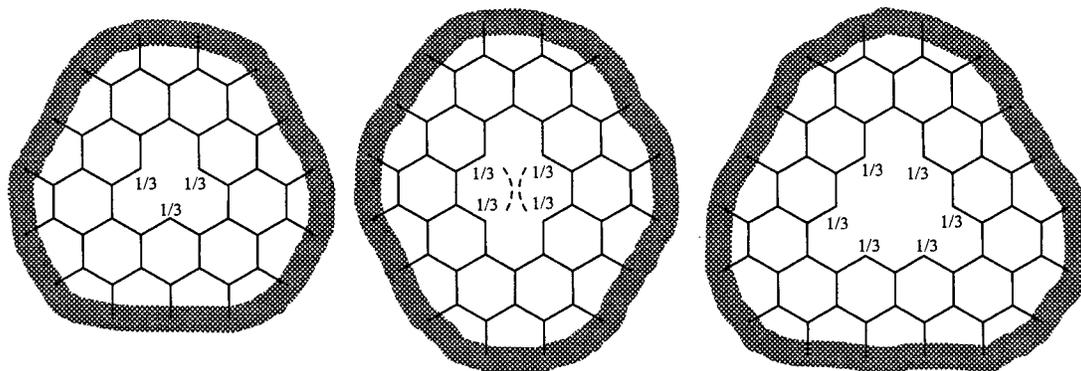
FIG. 16. Illustration of anti-methyl, anti-ethylene, and anti-allyl vacancy defects in a graphite lattice. The zeroth-order free valences are given and higher order spin pairings are indicated, so that the corresponding higher-order in the case of anti-ethylene becomes 0, while the net amount of unpaired electrons in the first and third cases remains 1 and 2, respectively.

VI. GRAPHITIC ANTI-MOLECULES

The question of the effect of local defect structures in otherwise perfect graphite may also be addressed. One may delete one or more contiguous carbon atoms from the graphite lattice, thereby giving what we term an *anti-molecule* corresponding to the molecule consisting of the internally still connected set of deleted atoms. Thus with deletion of a single C atom we obtain "anti-methyl," and with deletion of two adjacent atoms we obtain "anti-ethylene," and with deletion of three consecutive atoms we obtain "anti-allyl." The resonance-theoretic predictions are relatively straightforward to make, as illustrated in Fig. 16. In fact one may perceive a general pattern. Note perfect graphite has a local balance of starred and unstarred sites, and note that in the formation of an anti-molecule я by deletion of the molecule R, the unbalance of starred and unstarred sites in the region of the anti-molecule must be the same (except maybe for sign) as the unbalance in the corresponding molecule R. That is, for methyl, ethylene, and allyl one has an unbalance of 1, 0, and 1, so that this should also be the regional unbalance in site types for anti-methyl, anti-ethylene, and anti-allyl, respectively, and this then leads to this consequent number of unpaired electrons, to be localized in the region of the corresponding defect (i.e., of the corresponding anti-molecule я). Thus for a general molecule R with numbers $\#_\star$ & $\#_\circ$ of starred and unstarred sites, our mean-field resonance theory predicts (at least) $|\#_\star - \#_\circ|$ defect-localized unpaired electrons for the corresponding anti-molecule я in graphite

$$\{\#я\text{-localized unpaired e}\} = \{|\#_\star - \#_\circ| \text{for R}\}. \quad (5)$$

Indeed this result of matching of properties (in particular of net spin densities) for the molecule and anti-molecule, in part justifies our choice of nomenclature of "anti-molecules" for our vacancy defects.

These predictions might be sought to be checked *via* an MO-theoretic approach. Of course with a local defect the translational symmetry of the graphite lattice is spoiled, so that ordinary band-theoretic computations are not directly applicable. Thus what one might do is simulate bulk graphite with "suitable" large fragments, and delete a few sites from the center of the fragment to represent the defect. But to do this in practice it is crucial to understand what fragments

might be "suitable"—in particular if we are to look for (near) nonbonding MOs associated to the defect, it would be preferable to avoid other near nonbonding MOs, such as could arise with certain fragment edges or corners. But in fact because of the preceding sections we understand how to choose suitable fragments. In particular an example of such a suitable fragment would have edges and corners of the first (or second) types indicated in Fig. 9, and we have now performed computations for about a dozen anti-molecules near the center of such a fragment, with $N = 684$ sites (before deleting the sites in the defect). Examination is made especially of the HOMO, and perhaps a few MOs nearby to $\epsilon = 0$ so as to ascertain their disposition in the defected fragment. The results of these examinations are indicated in Fig. 17, where there are plotted logarithms of mean MO densities as a function of the graphical distance from the center of the central hexagon whereat the defect is placed. When there are several degenerate nonbonding MOs these plots use the average densities for these different orbitals, and when there are no nonbonding MOs the plot shows the density for the HOMO. At the top of each plot a depiction of the anti-molecule я is shown in bold, with a lighter hexagon showing the position of я with respect to the central hexagon of the fragment. And yet further with each plot there is indicated the values of the orbital energies ϵ_i for the orbitals which are plotted, and in addition in parentheses, there are shown the energies ϵ_j for the next orbital away (from the perfectly nonbonding $\epsilon = 0$ value). Upon examination of the results in this Fig. 17, one sees that the orbital densities for the orbitals anticipated to correspond to unpaired electrons, indeed generally have nonbonding energy, and in fact this must be the case since for the finite fragments used, with equal numbers of ★ and ○ sites before deletion of the defect, the Coulson–Rushbrooke theorem[34] implies that the unbalance of ★ and ○ in the defected fragment must match the unbalance of the deleted molecule R. The remaining orbitals (not so implied to be $\epsilon = 0$) are always distinctly different in energy from $\epsilon = 0$, as perhaps could be surmised from the relatively large HOMO–LUMO gap in the undefected fragment. Moreover the nonbonding ($\epsilon = 0$) orbitals seem to be more localized in the region of the defect. In the cases (as anti-ethylene, anti-butadiene, and anti-benzene) where no such defect-localized
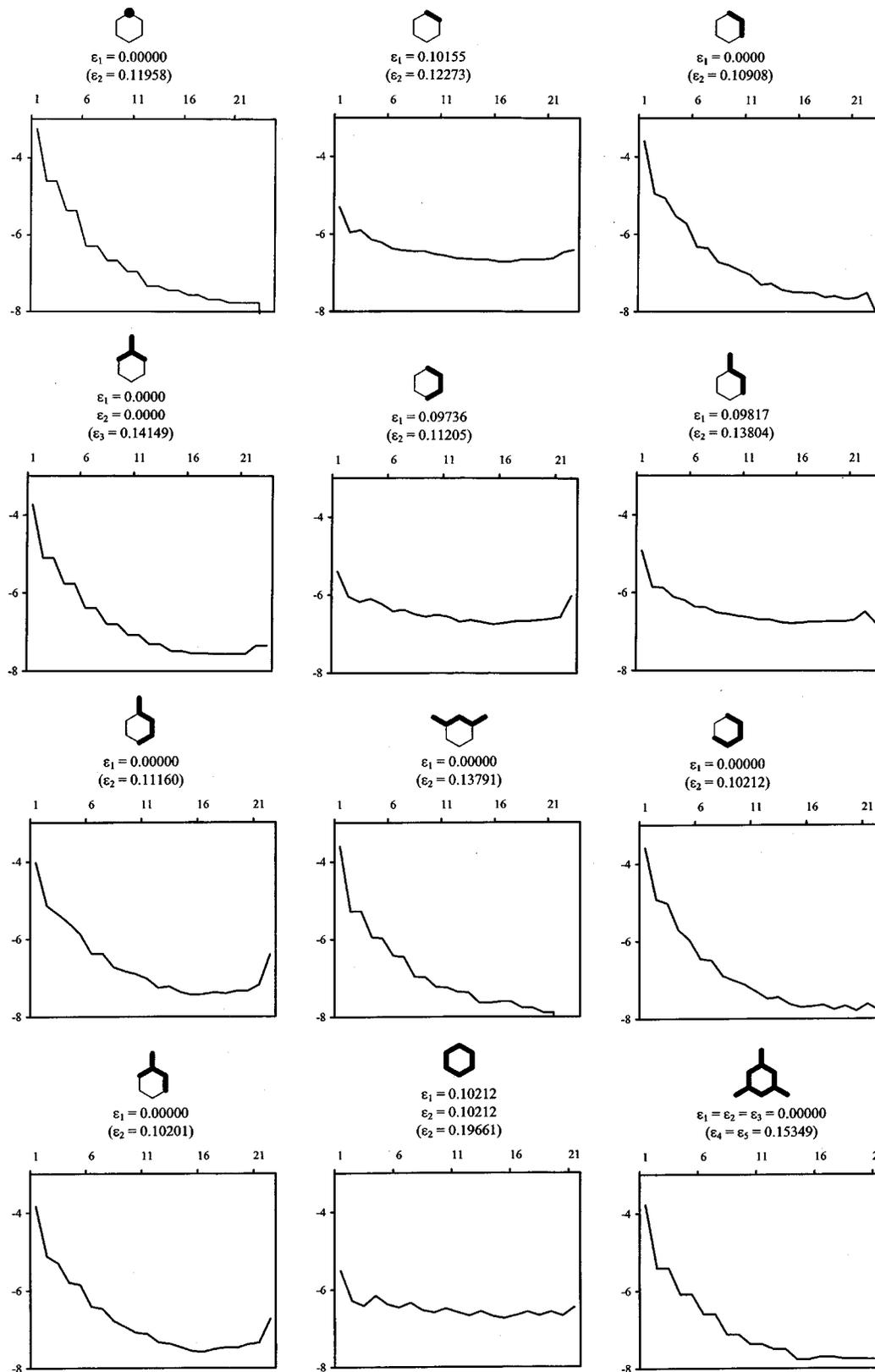
FIG. 17. Mean HOMO (or near-HOMO) densities for several anti-molecules, plotted as a function of the shortest-path distance from the defect. The anti-molecule defect structure is indicated in boldface, while the central hexagon of the erstwhile hexagonal-symmetry fragment is indicated in lighter face, and the energies of the more nearly nonbonding MOs is also given (those not enclosed in parentheses being those for which the mean densities are plotted).

orbitals are expected, one sees that in fact the most nearly nonbonding MOs are in fact markedly more delocalized (i.e., more nearly constant, as gauged by the functional dependence of their average density on the distance from the center of the fragment). The decay of the $\epsilon = 0$ orbital densities away from the defect appears only roughly exponential, there evidently being some degree of interaction with the edges of the fragment, as does not seem to unreasonable since the

present distances here are: first, somewhat smaller than the distances between strip edges which involved the nice exponential decay of Fig. 8; and second, several times (~10) smaller than the distance between polymer ends where the dramatic exponential decay of Fig. 15 was observed. Still it appears that the number of such nonbonding defect-localized MOs generally exactly matches what is anticipated from our mean-field resonance theory—i.e., the number of such MOs for an anti-molecule is just $|\#_\star - \#_\circ|$ for the corresponding molecule.

Thus our mean-field resonance theory seems to correctly predict significant characteristics of these various anti-molecules. Also it may be mentioned that the resonance theory frequently predicts that the unpaired electrons lie predominantly on one type of site ($\star$ or $\circ$), and though not shown in Fig. 17 because of the local averaging, the MO computations then generally find the defect localized nonbonding MOs on the same type of sites. Thus general agreement is obtained between our MO computations and the resonance-theoretic predictions.

VII. CONCLUSION

The simple resonance-theoretic scheme advocated here seems to make quite reasonable predictions as to amount and location of spin density. Beyond general agreement with other VB-theoretic spin predictions[27–33] for small molecules, the general predictions have here been tested against more quantitative MO-based predictions for several extended systems: About two dozen graphitic edges, a more limited number of graphitic corners and polymer ends, and about a dozen "anti-molecule" vacancy defects. The uniformity of agreement of the resonance-theoretic predictions with the results of the MO-theoretic computations enhances the credence of the predictions. Especially dramatically for edges and anti-molecules we have the essentially quantitative predictions of Eqs. (4) and (5). That is, we have identified accurately the number of nonbonding nondelocalized orbitals thereby revealing a systematic pattern of behavior for these edges and anti-molecules. Also the general qualitative predictions for the other cases (e.g., the corners) and as regards the location of the unpaired spin density seems to be in agreement between the two approaches.

It may be noted that there are several other earlier MO-theoretic computations for which some data has been reported,[42] and which seem to be in "rough" agreement with the predictions of our simple resonance-theoretic scheme. The agreement is often rough because it may be that there is not sufficient information reported to reconstruct all the desired correspondences, or because there is a gradation of orbitals from localized to delocalized (and correspondingly from nonbonding to less nonbonding). Some aspects of this problem were revealed in our discussion of the third and fourth types of corners in Fig. 9, and further aspects concerning the gradation of bonding strengths (and associated localization) for the oft-considered case of hexagonal fragments, as in Fig. 12. In such cases the partitioning into bonding and nonbonding is not so clear cut. But our resonance-theoretic approach still readily makes the prediction that such gradations occur, and indeed we again note that the resonance-

theoretic predictions seem generally to be in rough agreement with numerous computations.[42] Some resonance-theoretic predictions as to fine splittings amongst weakly spin paired electrons have not been gone into because of generally accepted inadequacies of the limited MO-based computations we have made, and these predictions naturally should be further addressed in future work. The prediction of the resonance theory as to whether unpaired electron density appears (primarily) on starred or unstarred sites seems to be correct (though we have not tried to display this so much in our numerical comparisons). For smaller molecules the locations of unpaired electron density beyond this aspect is difficult with the present qualitative resonance theory (e.g., because of the "interaction" between different edges which are necessarily nearby in such species).

A few words of qualification should be included, particularly as regards non-benzenoid conjugated hydrocarbons. The resonance theory as developed here need not apply so well to systems with cyclobutadiene moieties, because: First, Pauling's resonance theory was developed to match to classical chemical ideas which were clearest for the benzenoids; second, there are well-known problems of predictions of resonance energies for cyclobutadiene (and related $4n$-cycle-containing species); and third, theoretically there are additional corrections beyond those of the nearest-neighbor Pauling–Wheland model for systems with small cycles. (In fact these last-mentioned corrections[43] are to accommodate the second-mentioned problems.) For nonalternant systems the manner of setting up our resonance theory clearly needs fundamental modification, since the alternant character is so intimately involved in our present formulation for the resonance structures (with pairing solely between sites of different types). For the various non-benzenoid conjugated networks (nonalternant or with $4n$-cycles), it is imagined that though resonance theory will still be applicable it should need some modification from what is presented here. Still the benzenoid case is of sufficient interest that the present formulation should be valuable—and also some applications[26] to selected small non-benzenoid molecules have been successful.

In conclusion it seems that the mean-field resonance-theoretic approach is of much qualitative value, giving insight to the effect of chemical structure on electron pairing and associated magnetic and conductive properties, all in the framework of traditional organic chemical ideas. The predictions are seen often to be especially neat for extended systems, where resonance theory has traditionally been less frequently applied. Particular interest arises: First since graphite is rich in various kinds of impurities or defects, the structures of which have seldom been well characterized; and second since with the advent of carbon nano-tubes, the question of various nano-structures thereon naturally arises. Thus beyond application to conventional ordinary molecules and polymers, the current mean-field resonance theory may be of especially notable aid in characterizing extended nano-structured systems and graphitic defect structures. It seems that traditional organic chemical reasoning may be neatly extended in a very easy to use format to understand a variety

of novel benzenoid π-conjugate networks, which are of ever increasing interest.

ACKNOWLEDGMENT

[1] J. W. Armit and R. Robinson, J. Chem. Soc. (London) **38**, 827 (1922).
[2] L. Pauling and G. W. Wheland, J. Chem. Phys. **1**, 362 (1933).
[3] L. Pauling, *The Nature of the Chemical Bond* (Cornell University Press, Ithaca, NY, 1939).
[4] G. W. Wheland, *Resonance in Organic Chemistry* (Wiley, New York, 1955).
[5] E. Clar, *The Aromatic Sextet* (Wiley, New York, 1972).
[6] O. Kahn, *Molecular Magnetism* (VCH, New York, 1993).
[7] *Magnetic Properties of Organic Materials*, edited by P. M. Lahti (Dekker, New York, 1999).
[8] J. H. Van Vleck and A. Sherman, Rev. Mod. Phys. **7**, 167 (1935).
[9] D. J. Klein, S. A. Alexander, W. A. Seitz, T. G. Schmalz, and G. E. Hite, Theor. Chim. Acta **69**, 393 (1986).
[10] W. T. Simpson, J. Am. Chem. Soc. **75**, 597 (1953).
[11] W. C. Herndon, J. Am. Chem. Soc. **95**, 2404 (1973); Thermochim. Acta **8**, 225 (1974).
[12] M. Randić, Tetrahedron **33**, 1905 (1977); J. Am. Chem. Soc. **99**, 444 (1977).
[13] D. J. Klein, J. Chem. Educ. **69**, 691 (1992).
[14] D. J. Klein, H. Zhu, R. Valenti, and M. A. Garcia-Bach, Int. J. Quantum Chem. **65**, 421 (1997).
[15] S. J. Cyvin and I. Gutman, *Kekule Structures in Benzenoid Hydrocarbons* (Springer-Verlag, Berlin, 1988).
[16] D. J. Klein and L. Bytautas, J. Phys. Chem. **103**, 5196 (1999).
[17] See, e.g., G. Urry, *Elementary Equilibrium Chemistry of Carbon* (Wiley, New York, 1989).
[18] G. Rumer, Göttinger Nach. Ges. Wiss. **1932**, 337.
[19] G. Rumer, E. Teller, and H. Weyl, Göttinger Nach. Ges. Wiss. **1932**, 499.
[20] There are many references where this is discussed (following that of Ref. 19); see, e.g., R. Pauncz, *Spin Eigenfunctions* (Plenum, New York, 1979).
[21] N. S. Ham and K. Ruedenberg, J. Chem. Phys. **29**, 1215 (1958).
[22] L. Pauling, sections 7.5 & 7.6 of the 3*rd* edition of Ref. 3; L. Pauling, Acta Crystallogr., Sect. B: Struct. Sci. **36**, 1898 (1980).
[23] W. C. Herndon and M. L. Ellzey, J. Am. Chem. Soc. **16**, 6631 (1974).
[24] See, e.g., P. Dowd, J. Am. Chem. Soc. **88**, 2587 (1966); J. Berson, *Diradicals*, edited by W. T. Borden (Wiley, NY, 1982), Chap. 4. P. G. Weinhold, J. Hu, R. R. Squires, and W. C. Lineberger, J. Am. Chem. Soc. **118**, 475 (1996).
[25] See, e.g., D. R. Yarkony and H. F. Schaeffer, III, J. Am. Chem. Soc. **96**, 3754 (1974). S. B. Auster, R. M. Pitzer, and M. S. Platz, *ibid.* **100**, 3812 (1982).
[26] D. J. Klein, pages 41–59 of Ref. 7.
[27] E. H. Lieb and D. C. Mattis, J. Math. Phys. **3**, 749 (1962).
[28] A. A. Ovchinnikov, Theor. Chim. Acta **47**, 297 (1978).
[29] D. J. Klein, J. Chem. Phys. **77**, 3098 (1982).
[30] E. H. Lieb, Phys. Rev. Lett. **62**, 1201 (1989).
[31] D. Döhnert and J. Koutecky, J. Am. Chem. Soc. **102**, 1789 (1980); D. J. Klein, C. J. Nelin, S. A. Alexander, and F. A. Matsen, J. Chem. Phys. **77**, 3101 (1982); J. Koutecky, D. Döhnert, P. E. S. Wormer, J. Paldus, and J. Cizek, *ibid.* **80**, 2244 (1984); S. A. Alexander, D. J. Klein, and M. Randić, Mol. Cryst. Liq. Cryst. **176**, 109 (1989); B. Sinha, I. D. L. Albert, and S. Ramasesha, Phys. Rev. B **42**, 9088 (1990).
[32] V. O. Cheranovskii, Teor. Eksp. Khim. **20**, 468 (1984). D. J. Klein and S. A. Alexander, in *Graph Theory & Topology in Chemistry*, edited by R. B. King & D. H. Rouvray (Elsevier, Amsterdam, 1987), pp. 404–419.
[33] See, e.g., W. T. Borden and E. R. Davidson, J. Am. Chem. Soc. **99**, 4587 (1977); P. Karafiloglou, J. Chem. Phys. **82**, 3728 (1985); P. Nachtigali and K. D. Jordan, J. Am. Chem. Soc. **115**, 270 (1993); K. Yoshizawa, M. Hatanaka, A. Ito, K. Tanaka, and T. Yamabe, Chem. Phys. Lett. **202**, 483 (1993).
[34] C. A. Coulson and G. S. Rushbrooke, Proc. Cambridge Philos. Soc. **36**, 193 (1940).
[35] D. J. Klein, Chem. Phys. Lett. **217**, 261 (1994).
[36] P. R. Wallace, Phys. Rev. **71**, 622 (1948); M. Bradburn, C. A. Coulson, and Rushbrooke, Proc. R. Soc. Edinburgh, Sect. A: Math. Phys. Sci. **62**, 336 (1948); C. A. Coulson and G. S. Rushbrooke, *ibid.* **62**, 350 (1948).
[37] C. A. Coulson and G. R. Baldock, Discuss. Faraday Soc. **8**, 27 (1950); M. Fujita, K. Wakabayashi, K. Nakada, and K. Kusakabe, J. Phys. Soc. Jpn. **65**, 1920 (1996).
[38] D. J. Klein, Rep. Mol. Theory **1**, 91 (1990); K. Wakabayashi, M. Fujita, K. Kusakabe, and K. Nakada, Czech. J. Phys. S4 **46**, 1865 (1996).
[39] K. Nakada, M. Fujita, K. Wakabayashi, and K. Kusakabe, Czech. J. Phys. S4 **46**, 2429 (1996); M. Nakada, M. Fujita, G. Dresselhaus, and M. S. Dresselhaus, Phys. Rev. B **54**, 17 954 (1996); K. Wakabayashi, M. Fujita, H. Ajiki, and M. Sigrist, *ibid.* **59**, 8271 (1999).
[40] F. J. Mallory, K. E. Butler, and A. C. Evans, Tetrahedron Lett. **37**, 7173 (1996); F. J. Mallory, K. E. Butler, A. C. Evans, E. J. Brondyke, C. W. Mallory, C. Yang, and A. Ellenstein, J. Am. Chem. Soc. **119**, 2119 (1997); A. J. Berresheim, M. Müller, and K. Müllen, Chem. Rev. **99**, 1747 (1999).
[41] D. J. Klein, T. G. Schmalz, W. A. Seitz, and G. E. Hite, Int. J. Quantum Chem. **19**, 707 (1986).
[42] S. E. Stein and R. L. Brown, Carbon **23**, 105 (1985); J. Am. Chem. Soc. **109**, 3721 (1987); in *Molecular Structure & Energetics*, edited by J. Liebman, and A. Greenberg (VCH, NY, 1987), Vol. 2, pp. 37–66; H. Hosoya, H. Kumazaki, K. Chida, M. Ohuchi, and Y.-D. Gao, Pure Appl. Chem. **62**, 445 (1990); H. Hosoya, Y. Tsukano, M. Ohuchi, and K. Nakada, Nat. Sci. Reports Ochanomizu Univ. **44**, 155 (1993); M. Randić, Y. Tsukano, and H. Hosoya, Nat. Sci. Reports Ochanomizu Univ. **45**, 101 (1994); N. N. Tyutyulkov, G. Madjarova, F. Dietz, and K. Müllen, J. Phys. Chem. B **102**, 10183 (1998); L. G. Bulusheva, A. V. Okotrub, D. A. Romanov, and D. Tomanek, Phys. Low-Dim. Struct. **3/4**, 107 (1998); F. Dietz, N. Tyutyulkov, O. Madjarova, and K. Müllen, J. Phys. Chem. (to be published).
[43] J. J. C. Mulder and L. J. Oosterhoff, Chem. Commun. **1970**, 305. W. J. van der Hart, J. J. C. Mulder, and L. J. Oosterhoff, J. Am. Chem. Soc. **94**, 5724 (1972); S. Kuwajima, *ibid.* **106**, 6496 (1984); R. D. Poshusta, T. G. Schmalz, and D. J. Klein, Mol. Phys. **66**, 317 (1989).